THE ASTROPHYSICAL JOURNAL, 227:422–432, 1979 January 15

INTERSTELLAR METHYL ALCOHOL

C. A. GOTTLIEB, JOHN A. BALL, ELAINE W. GOTTLIEB, AND DALE F. DICKINSON
Harvard-Smithsonian Center for Astrophysics
Received 1978 June 22; accepted 1978 July 28

ABSTRACT

We observed CH_3OH by its $J = 2 \rightarrow 1$ rotational transitions at 96.7 GHz toward 14 galactic sources. We detected $^{13}CH_3OH$ and CH_3OD toward Sgr B2 and calculated values for the integrated intensity ratios. CH_3OH emission at 834 MHz in the galactic-center region is extended with respect to the $\sim 40'$ telescope beamwidth, although the column density of CH_3OH molecules peaks near Sgr A and Sgr B2. The CH_3OH column densities are less than or $\sim 6 \times 10^{14}$ cm^{-2} except toward Sgr B2 ($\sim 2 \times 10^{16}$ cm^{-2}), 3′ south of Sgr A (3×10^{15} cm^{-2}), and toward the Kleinmann-Low nebula ($\sim 2 \times 10^{15}$ cm^{-2}) in Orion. The $^{12}CH_3OH$ spectra at 96.7 GHz yielded collision rates. We compared the angular extent and column densities of CH_3OH and H_2CO and critically examined the recently proposed formation schemes for CH_3OH.

Subject headings: interstellar: abundances — interstellar: molecules

I. INTRODUCTION

Methyl alcohol (CH_3OH) was detected at 834 MHz toward the galactic center by Ball *et al.* (1970) and subsequently observed at approximately 30 transitions toward Orion and 20 transitions toward Sgr B2.[1] Attempts to detect methyl alcohol in other galactic molecular sources were unsuccessful (see Buxton *et al.* 1977), except for the detection of the $J = 3 \rightarrow 2$ transition toward DR 21(OH) (Kutner *et al.* 1973). Because so little work, either observational or theoretical, has been done on the formation in interstellar clouds of polyatomic molecules containing five or more atoms, much can be learned from studies of such compounds and from comparisons with chemically related species.

[1] A molecule is assumed to be made up of its most abundant (terrestrial) nuclear species. Thus for $^{12}CH_3{}^{16}OH$ we write CH_3OH, and for $^{13}CH_3{}^{16}OH$ we write $^{13}CH_3OH$.

Our detailed observations of methyl alcohol establish it as a remarkably abundant molecule found in most galactic molecular clouds. Our observations are primarily of emission from the $J = 2 \rightarrow 1$ rotational transitions at 96.7 GHz with supporting data at 834 MHz of the $1_{10} \rightarrow 1_{11}$ (A) transition toward the galactic center. The CH_3OH emission we observed is in extended molecular clouds in contrast to emission from relatively high-lying states from sources less than or equal to 1′ in angular extent observed toward Orion (see Barrett *et al.* 1976 for a summary) and Sgr B2 (Zuckerman *et al.* 1972; Turner, Gordon, and Wrixon 1972).

II. EQUIPMENT

Table 1 shows the molecular and system parameters. We observed the $J = 2 \rightarrow 1$ transitions of $^{12}CH_3OH$, $^{13}CH_3OH$, and CH_3OD with the 36 foot (11 m) radio

TABLE 1

MOLECULAR AND SYSTEM PARAMETERS

Line	Rest Frequency* (MHz)	Transition	Species	Telescope Diameter (m)	Dates of Observations	T_{syst}† (K)
	834.267 ± 0.002	$1_{10} \rightarrow 1_{11}$ A	$^{12}CH_3OH$	43	1973 June 3–8	155
	90,703.78 ± 0.05‡	$2_{-1} \rightarrow 1_{-1}$ E	CH_3OD	11	1975 May 5–11	...
	90,705.77 ± 0.05‡	$2_0 \rightarrow 1_0$ A			1978 February 18	770
	90,743.60 ± 0.05‡	$2_1 \rightarrow 1_1$ E				
	94,405.17 ± 0.17	$2_{-1} \rightarrow 1_{-1}$ E	$^{13}CH_3OH$	11	1977 July 26	780
	94,407.02 ± 0.10	$2_0 \rightarrow 1_0$ A			1978 February 18	735
	94,410.76 ± 0.10	$2_0 \rightarrow 1_0$ E				
	94,420.36 ± 0.15	$2_1 \rightarrow 1_1$ E				
1	96,739.39 ± 0.10	$2_{-1} \rightarrow 1_{-1}$ E	$^{12}CH_3OH$	11	1977 July 21–27	680
2	96,741.42 ± 0.10	$2_0 \rightarrow 1_0$ A				
3	96,744.58 ± 0.10	$2_0 \rightarrow 1_0$ E				
4	96,755.51 ± 0.10	$2_1 \rightarrow 1_1$ E				

* Lees *et al.* (1973) unless otherwise noted.

† Approximate single-sideband system temperature.

‡ Suenram and Lovas (personal communication).

telescope of the National Radio Astronomy Observatory[2] (NRAO) at Kitt Peak, Arizona. We used the 80 to 120 GHz cooled mixer receiver with 256 1.0 MHz, 0.5 MHz, 0.25 MHz, and 0.10 MHz filters. A chopper wheel calibrated these observations. For most $^{12}CH_3OH$ and all $^{13}CH_3OH$ observations, we used the tunable Fabry-Perot filter constructed by Wannier *et al.* (1976). We made the 1975 May CH_3OD observations at 90.7 GHz without the Fabry-Perot filter, but we repeated these observations in 1978 February with the filter to determine the strength of the strong HNC feature which is 43 MHz lower in frequency. Since we found excellent agreement between these two sets of observations, we did not adjust the CH_3OD temperature scale. Our observations of $^{12}CH_3OH$ at 96.7 GHz with and without the filter show that the uncertainty in the temperature scale is only about 10% without the filter at this frequency.

Because of difficulties in reading one of the magnetic tapes recorded at the telescope in 1977 July, we digitized some of the spectra by scanning them with a Mann measuring engine. Tests showed that no appreciable error was introduced in the digitizing process.

At 36 cm (834 MHz) we observed with the 140 foot (43 m) telescope of NRAO at Green Bank, West Virginia. We used a room-temperature parametric amplifier and a broad-band dipole feed which accepted linear polarization. We inferred an aperture efficiency of ~31% from measurements of Virgo A for which we assumed a flux of 307.5 Jy at 834 MHz. Because of this lower aperture efficiency, the methanol profiles toward Sgr A and Sgr B2 are correspondingly weaker than those reported by Ball *et al.* (1970). The antenna beamwidths in the E and H planes were 42′ and 38′. We used the 413-channel autocorrelation receiver in the total power mode.

[2] The National Radio Astronomy Observatory is operated by Associated Universities, Inc., under contract with the National Science Foundation.

III. OBSERVATIONS

Four $J = 2 \rightarrow 1$ (A, E) transitions near 96.7 GHz are observable simultaneously with the 0.25 MHz and 0.10 MHz filter bank receivers. Our CH_3OH spectrum toward Orion (OMC 1) is in Figure 1; four vertical bars represent the positions of the four transitions (refer to the inset for the positions of these transitions on the CH_3OH energy level diagram). The relative strengths of the vertical bars come from the model described in § IV. Using the line widths and Doppler velocities in Table 2, we superposed the calculated Gaussian profiles on the observed spectra.

We also detected the $J = 2 \rightarrow 1$ transitions toward W3(OH), NGC 1333, Orion (OMC-2), NGC 2024, NGC 2264, ρ Oph, Sgr A, Sgr B2, M17 SW, W49, W51, DR 21(OH), and NGC 7538. Representative spectra are shown in Figures 2 and 3, and the parameters are summarized in Table 2.

The spectra in Figures 1, 2, and 3 reveal certain general properties which we summarize as follows:

1. The $2_{02} \rightarrow 1_{01}$ A transition is always the strongest of the four $J = 2 \rightarrow 1$ transitions.

2. The peak strength is ~1 K except in Orion OMC-1 ($T_A^* \sim 2$ K), Sgr B2 ($T_A^* \sim 3$ K), Sgr A ($T_A^* \sim 2$ K), and W49 ($T_A^* \sim 0.3$ K).

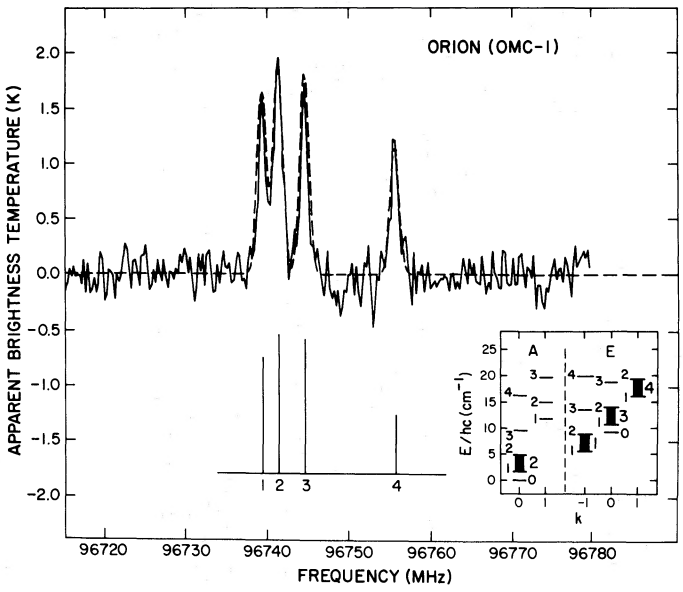

FIG. 1.—$^{12}CH_3OH$ spectrum toward the Kleinmann-Low nebula in Orion A with 0.775 km s^{-1} resolution. A linear baseline was subtracted. The frequency scale is based on an assumed velocity with respect to the local standard of rest of 8.3 km s^{-1}. The positions of the four transitions within the spectral window are labeled as in the energy level diagram (see inset in the lower right-hand corner). The relative strengths of the four transitions come from the model discussed in the text. We obtained the theoretical profiles superposed on the observed spectrum (*solid curve*) by representing the individual transitions with Gaussians whose full width at half-maximum is 4.1 km s^{-1}. The dashed curve is the theoretical spectrum.

TABLE 2

$^{12}CH_3OH$ EMISSION FEATURES

SOURCE	POINTING POSITION (1950)		T_A^* (K)				V_{LSR}† (km s^{-1})	ΔV‡ (km s^{-1})	RESOLUTION (km s^{-1})
	α	δ	$2_{-1} \rightarrow 1_{-1}\, E$	$2_0 \rightarrow 1_0\, A^*$	$2_0 \rightarrow 1_0\, E$	$2_1 \rightarrow 1_1\, E$			
W3(OH).....	2^{h}23^{m}17^s.0	61°39′00″.0	0.31	0.62 ± 0.05	0.17	< 0.18	−46.6 ± 0.2	4.7 ± 0.6	0.7747
NGC 1333.....	3 26 00.0	31 05 00.0	0.76§	0.84 ± 0.20§	< 0.4§	< 0.4§	9.4 ± 0.1	1.5 ± 0.4	0.7747
Orion A.....	5 32 46.8	−05 24 24.0	1.55	1.87 ± 0.09	1.61	1.12	8.3 ± 0.1	4.1 ± 0.2	0.7747
OMC − 2.....	5 33 00.0	−05 12 34.0	< 0.5	0.70 ± 0.10	< 0.3	< 0.4	10.8 ± 0.2	1.4 ± 0.4	0.3099
NGC 2024.....	5 39 12.0	−01 55 42.0	0.80	0.85 ± 0.09	< 0.3	< 0.3	10.48 ± 0.09	1.7 ± 0.2	0.3099
NGC 2264.....	6 38 28.0	09 32 12.0	0.96‖	1.33 ± 0.11‖	< 0.34‖	< 0.34‖	7.3 ± 0.2	3.2 ± 0.4	0.7747
ρ Oph.....	16 23 22.0	−24 16 20.0	< 0.3	0.70 ± 0.10	< 0.3	< 0.3	3.5 ± 0.2	1.6 ± 0.4	0.7747
M17 SW.....	18 17 28.0	−16 15 00.0	0.44	0.70 ± 0.07	0.29	< 0.2	20.3 ± 0.2	3.5 ± 0.5	0.7747
W49.....	19 07 50.0	09 01 18.0	0.3#	0.2 ± 0.15#	< 0.15#	< 0.15#	...	...	0.7747
W51.....	19 21 27.0	14 24 39.0	1.31**	0.9**	0.55**	≤0.24**	56.6 ± 0.6††	8.4 ± 2††	0.7747
DR 21(OH).....	20 37 14.0	42 12 00.0	0.86	1.16 ± 0.07	0.38	< 0.3	−2.6 ± 0.1	4.3 ± 0.4	0.7747
NGC 7538.....	23 11 37.0	61 11 48.0	0.62	1.01 ± 0.09	< 0.3	< 0.3	−56.3 ± 0.1	3.0 ± 0.3	0.7747

* Uncertainties are ±1 σ as determined by a least squares fit to the data of a linear baseline and Gaussian profiles and are representative of the uncertainties for the other three transitions.

† Doppler velocity referred to the local standard of rest and the $2_0 \rightarrow 1_0\, A$ line rest frequency in Table 1.

‡ Full width to half-maximum for the $2_0 \rightarrow 1_0\, A$ feature uncorrected for instrumental resolution.

§ Observed without the Fabry-Perot filter.

‖ The temperature scale has been multiplied by 1.6 because the spectrum was observed through the telescope dome.

Spectrum was too weak to fit with Gaussian profiles.

** The features could not be represented by Gaussian profiles.

†† Estimated from the $2_0 \rightarrow 1_0\, E$ feature.

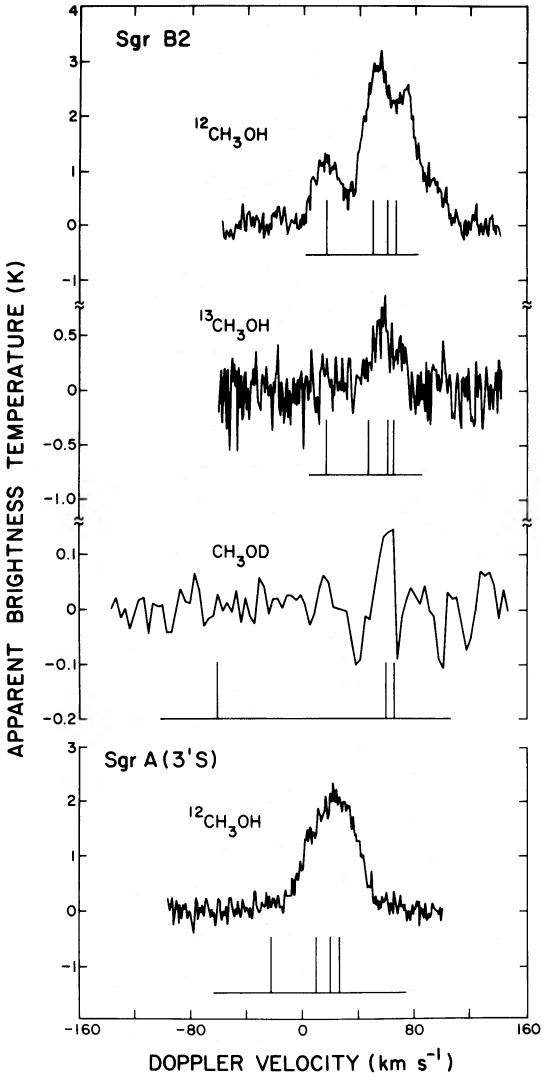

FIG. 2.—Spectra of $^{12}CH_3OH$, $^{13}CH_3OH$, and CH_3OD observed toward Sgr B2 and $^{12}CH_3OH$ observed 3′ south of Sgr A. The instrumental resolution is 0.25 MHz in the $^{12}CH_3OH$ and $^{13}CH_3OH$ spectra and 1 MHz in the CH_3OD spectrum. The expected positions of the four $J = 2 \rightarrow 1$ transitions in $^{12}CH_3OH$ and $^{13}CH_3OH$ and the three transitions in CH_3OD are indicated for a velocity of 60 km s^{-1} for Sgr B2 and a velocity of 20 km s^{-1} for $^{12}CH_3OH$ toward Sgr A (3′S). Linear baselines were subtracted.

3. The ratio of $2_{-1} \rightarrow 1_{-1} E$ to $2_{02} \rightarrow 1_{01} A$ is between 0.5 and 1.

4. The $2_0 \rightarrow 1_0 E$ transition is always less intense than $2_{02} \rightarrow 1_{01} A$.

5. The $2_1 \rightarrow 1_1 E$ transition was detected only in Sgr B2, Orion OMC-1, and possibly W51, although more integration might reveal this transition in the W3(OH), and DR 21(OH) spectra as well.

6. $^{13}CH_3OH$ and CH_3OD were detected in Sgr B2 only.

In the following subsections we describe in more detail our spectra toward the galactic-center region, including the observations of $^{13}CH_3OH$ and CH_3OD in Sgr B2, and some preliminary mapping results toward the Orion molecular cloud.

a) Sagittarius B2

Figure 2 shows the $^{12}CH_3OH$, $^{13}CH_3OH$, and CH_3OD spectra on a common velocity scale based on the $2_{02} \rightarrow 1_{01} A$ rest frequency for each molecular species. In the $^{12}CH_3OH$ and $^{13}CH_3OH$ spectra four $J = 2 \rightarrow 1$ transitions occur in the spectrometer bandwidth, but only two CH_3OD transitions ($2_{02} \rightarrow 1_{01} A$ and $2_{-1} \rightarrow 1_{-1} E$) occur this close in frequency ($2_0 \rightarrow 1_0 E$ is within the HNC line width and $2_1 \rightarrow 1_1 E$ is ~ 38 MHz higher in frequency). The identification of the feature in Figure 2 with CH_3OD rests only on the close coincidence in frequency between the astronomical line and the laboratory-measured rest frequency. The CH_3OD feature is 42.2 MHz higher than the strong HNC feature and thus would be at -80 km s^{-1} if it were HNC. Since ^{12}CO exists at -80 km s^{-1} (Turner *et al.* 1978), we cannot definitely rule out HNC at -80 km s^{-1}. Unfortunately, observation of CH_3OD is difficult because it occurs in a region where the third harmonic of the paramp oscillator can affect the baseline.

In the center portion of the $^{12}CH_3OH$ and $^{13}CH_3OH$ spectra, three blended rotational transitions occur with separations of 6.3 and 9.8 km s^{-1} that are less than the turbulently broadened Doppler width of ~ 20 km s^{-1}. The $^{12}CH_3OH$ spectrum is further complicated by what might be self-absorption at the center of the profile. However, the $2_1 \rightarrow 1_1 E$ transition is sufficiently displaced in frequency from the other three transitions to be resolved, does not show self-absorption even in the $^{12}CH_3OH$ spectrum, and is probably optically thin. The $^{13}CH_3OH$ and CH_3OD profiles are also narrower in velocity than the $^{12}CH_3OH$ profile.

We did not fit the central portion of the $^{12}CH_3OH$ and $^{13}CH_3OH$ spectra with Gaussian profiles because the three transitions in $^{12}CH_3OH$ and $^{13}CH_3OH$ are blended, and the relative strengths are not easily estimated from theory. We compare instead the peak brightness temperature and integrated line intensities. Table 3 shows the peak brightness temperatures for $^{12}CH_3OH$, $^{13}CH_3OH$, and CH_3OD and the ratio of integrated line intensities

$$R(^{13}CH_3OH/^{12}CH_3OH) = \int I(^{13}CH_3OH)dv \Big/ \int I(^{12}CH_3OH)dv ,$$

and $R(CH_3OD/^{13}CH_3OH)$ (where the integrals extend over the entire detectable profiles).

The ratio $R(^{13}CH_3OH/^{12}CH_3OH)$ in Sgr B2 is ~ 3 times less than the ratio of peak strengths, but about 10 times larger than the terrestrial $^{13}C/^{12}C$ ratio. This implies that the $^{12}CH_3OH$ is optically thick, consistent with the possible presence of a self-absorption dip near the center of the $^{12}CH_3OH$ profile. The ratio

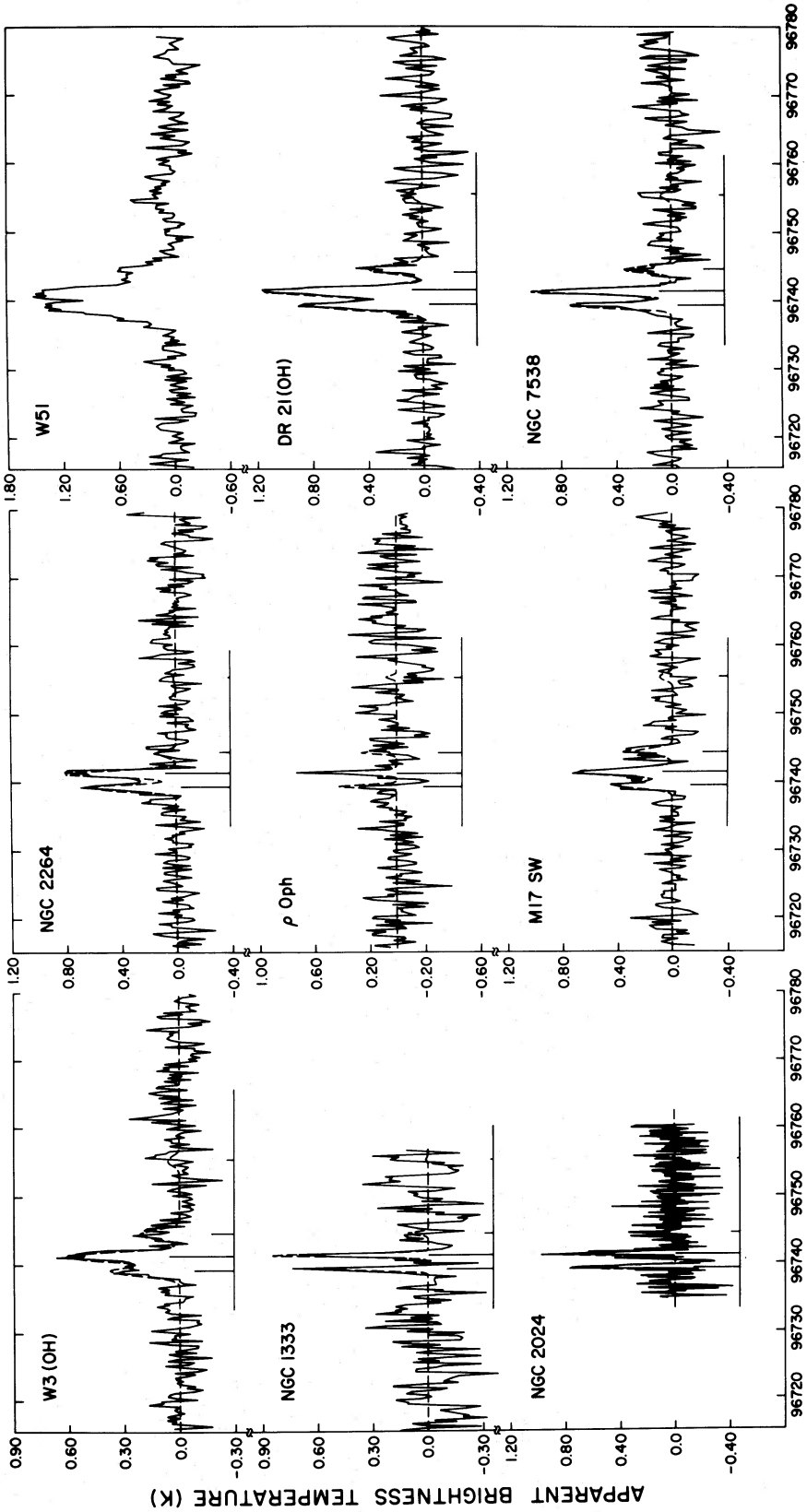

FIG. 3.—$^{12}CH_3OH$ spectra toward nine galactic sources. The instrumental resolution is 0.3099 km s^{-1} for NGC 2024 and 0.775 km s^{-1} for the other sources. The pointing positions and Doppler velocities are given in Table 2. The NGC 2264 spectrum is uncorrected for attenuation by the telescope dome. All other comments under Fig. 1 apply.

TABLE 3

PEAK BRIGHTNESS TEMPERATURES AND INTEGRATED INTENSITY RATIOS

SOURCE	PEAK T_A* (K)			INTEGRATED INTENSITY RATIOS*	
	$^{12}CH_3OH$	$^{13}CH_3OH$	CH_3OD	$R(^{13}CH_3OH/^{12}CH_3OH)$	$R(CH_3OD/^{13}CH_3OH)$
Orion A.....	1.87 ± 0.09	≤0.2	...	≤0.1	...
Sgr B2.....	3.1 ± 0.2	0.8 ± 0.3	0.14 ± 0.06	0.10 ± 0.02	0.09 ± 0.03

* Quoted errors are the ±1 σ statistical uncertainties due to noise.

$R(CH_3OD/^{13}CH_3OH)$ is a lower limit, since the $2_0 \rightarrow 1_0$ E transition in CH_3OD is not in the integral

$$\int I(CH_3OD)dv .$$

b) Sagittarius A

The $^{12}CH_3OH$ spectrum in Figure 2, observed 3′ south of Sgr A, shows a single broad, nearly structureless profile centered on the group of three closely spaced transitions. Unlike the $^{12}CH_3OH$ spectrum in Sgr B2, there is no evidence of the $2_1 \rightarrow 1_1$ E transition and no hint of self-absorption.

c) Orion

We hoped to compare CH_3OH with 2 mm H_2CO emission studied by Kutner, Evans, and Tucker (1976). We established that the CH_3OH emission at 96.7 GHz is extended by detecting CH_3OH emission at the KL nebula and OMC-2 positions and at positions 1′ N, 2′ N, 4′ N, 2′ S, 4′ S, 2′ E, and 2′ W of the KL position. Therefore CH_3OH emission at 96.7 GHz is definitely extended in contrast to CH_3OH emission at 1 cm, which is observed only at the KL position (Hills, Pankonin, and Landecker 1975).

Orion was close to the Sun, and the surface humidity was high when we attempted to map the CH_3OH in 1977 July. These conditions caused the receiver to be unstable and resulted in bad spectrometer baselines; our CH_3OH map should be redone under more favorable observing conditions. At positions offset from KL, T_A* < 1 K (except possibly at the 2′ N position), so mapping CH_3OH is a slow process. Our CH_3OH map appears to have boundaries similar to the H_2CO emission reported by Kutner, Evans, and Tucker (1976).

Since $^{13}CH_3OH$ was not detected in Orion, only an upper limit for $R(^{13}CH_3OH/^{12}CH_3OH)$ is given in Table 3. If the $^{12}CH_3OH$ is optically thin, then our upper limit is consistent with the $^{12}C/^{13}C$ ratio of 25 ± 5 estimated by Gottlieb *et al.* (1975) from HCN or ~77 estimated by Kutner, Evans, and Tucker (1976) from studies of H_2CO.

d) Map of the Galactic-Center Region at 36 cm

We also mapped the 36 cm $1_{10} \rightarrow 1_{11}$ A K-type doublet line toward the galactic-center region. Barrett *et al.* (1972) mapped the central portion of the Sgr B2 molecular cloud in the $J = 1 \rightarrow 0$ methanol transitions. This is the only previous information on the angular extent of these methanol clouds. Although the angular resolution of our 36 cm map is coarse (~40′), we were able to sample a large enough area to compare with the 6 cm formaldehyde absorption toward the same region.

Table 4 and Figure 4 show the results of mapping the 36 cm line at approximately half-beamwidth spacings. Between $l^{II} = 359.^{\circ}665$ and $l^{II} = 0.^{\circ}952$ ($b^{II} = -0.^{\circ}04$) we detected methanol emission at all points probed. We also detected methanol emission both above and below the galactic plane along lines centered at Sgr A and Sgr B2. The integrated intensity and the continuum temperature, T_c, at nine positions near the galactic plane are in Table 4.

The integrated intensity divided by T_c, and thus the number of methanol molecules, peaks toward Sgr A and Sgr B2. T_L/T_c is nearly constant at about 10^{-3}, therefore the 36 cm line is probably optically thin. Qualitatively these observations are similar to the

TABLE 4

METHANOL EMISSION AT 834 MHz IN THE GALACTIC-CENTER REGION

POINTING POSITION (1950)				INTEGRATED INTENSITY (K km s^{-1})	T_c (K)	INTEGRATED INTENSITY/T_c (km s^{-1})
α	δ	l^{II}	b^{II}			
$17^h41^m20^s.2$	−28°49′29″...	359.°954	+0.°254	5 ± 1	198 ± 20	0.025 ± 0.008
17 41 45.7	−29 13 22...	359.665	−0.035	8 ± 1	212 ± 21	0.04 ± 0.01
17 42 28.0	−28 58 30...	359.954	−0.035	13 ± 1	247 ± 25	0.05 ± 0.01
17 43 03.5	−28 13 29...	0.663	+0.248	1.8 ± 0.4 2.5 ± 0.4	109 ± 11	0.04 ± 0.02
17 43 29.3	−28 37 20...	0.374	−0.041	6.8 ± 0.6	187 ± 19	0.036 ± 0.007
17 43 35.0	−29 07 43...	359.954	−0.324	9 ± 1	220 ± 22	0.041 ± 0.009
17 44 11.0	−28 22 30...	0.663	−0.041	7.1 ± 0.8	122 ± 12	0.06 ± 0.01
17 44 51.7	−28 07 46...	0.952	−0.041	1.9 ± 0.5	104 ± 10	0.018 ± 0.007
17 45 17.9	−28 31 36...	0.663	−0.330	7 ± 2	121 ± 2	0.06 ± 0.02

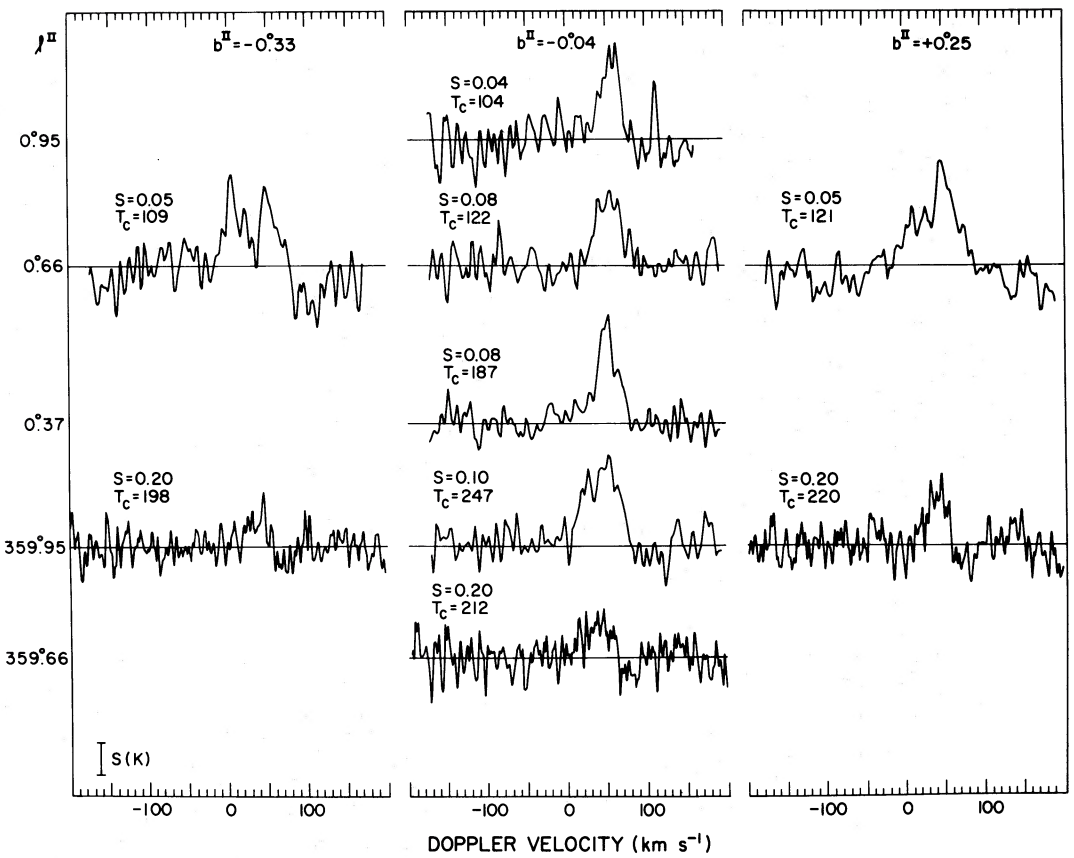

FIG. 4.—CH_3OH spectra at 834 MHz from l^{II} = 359°.665 to 0°.952 (b^{II} = −0°.04) and l^{II} = 359°.954 to 0°.663 at b^{II} = −0°.33 and +0°.25. The quantity S listed on the upper left-hand side of the profile determines the antenna temperature that is equal to the vertical bar at the lower left. The continuum antenna temperature T_c at each point is listed below the quantity S.

more detailed observations of 6 cm H_2CO absorption (Scoville *et al.* 1972), and ^{12}CO emission (Solomon *et al.* 1972; Scoville *et al.* 1974).

e) Sources in Which CH_3OH *Was Not Detected*

Table 5 contains upper limits to the CH_3OH emission at 96.7 GHz, although in two sources (M78 and CRL 2345) weak features were possibly present. Lada *et al.* (1974) and Gottlieb *et al.* (1978*a*) studied the subfragments M78 and NGC 2071 in dust cloud L1630 by using 2 mm H_2CO emission. The H_2CO emission toward these subfragments is comparable to that toward NGC 1333 from which we detected CH_3OH. We were surprised, then, to be unable to find CH_3OH toward M78 and NGC 2071.

IV. DISCUSSION

a) Abundances

i) *Method*

We solved the equations of statistical equilibrium in the optically thin case for the 40 lowest states in the *A* and *E* ladders. We used the line strengths and radiative rates calculated by Dr. M. M. Litvak (personal communication) for the asymmetric internal rotor. The results are close to those cited by Lees *et al.* (1973) and Lees (1973). We treated the *A* and *E* ladders independently, since there is no evidence in the data for unequal population between the two ladders. The kinetic temperature comes from ^{12}CO measurements (see Gottlieb *et al.* 1978*b*). We assumed that the incident radiation is isotropic and has a temperature of 2.7 K, and in sources outside the galactic-center region that the optical depth is less than 1 for the millimeter wavelength methanol lines (see §§ III*a* and *c*).

At wavelengths greater than or equal to 10 cm, the radiation temperature in the methanol clouds is probably greater than 2.7 K. Since the rates for induced emission and absorption for the long wavelength transitions are small, this assumption introduces no important uncertainties in the analysis.

In treating collisions we considered two limiting cases: (1) all collisional de-excitation rates between pairs of levels are the same; and (2) the collisional de-excitation rates are proportional to the electric dipole line strengths divided by the degeneracy of the upper level. In the actual analysis of the data we used collision case 2, but the following four tests were performed

TABLE 5

UPPER LIMITS TO $^{12}CH_3OH$ EMISSION AT 96.7 GHz

SOURCE	POINTING POSITION (1950) α	POINTING POSITION (1950) δ	UPPER LIMIT* (K)	V_{LSR}† (km s^{-1})	INSTRUMENTAL RESOLUTION (km s^{-1})
W3 (IRS 4)	02^{h}21^{m}44^s.0	+61°52′48″	≤0.44	−42.5	0.775
W3 (IRS 5)	02 21 53.0	+61 52 21	≤0.54	−34.8	0.775
M78	05 43 35.2	−00 13 00	≤0.80*	+10.2	0.775
NGC 2071	05 44 30.3	+00 21 48	≤0.65	+9.8	0.775
B227	06 04 31.0	+19 28 30	≤0.42	−0.4	0.775
IRC +10216	09 45 14.8	+13 30 40	≤0.42	−23.2	0.775
L134	15 51 00.0	−04 26 57	≤0.47	+3.0	0.3099
	15 51 02.0	−04 33 34	≤0.59	+3.0	0.3099
L134 N	15 51 28.0	−02 45 00	≤0.77	+3.0	0.3099
CRL 2341	19 11 06.4	+10 48 24	≤0.26	+55.0	0.775
CRP 2345	19 12 00.0	+11 04 00	≤0.41*	+56.0	0.775
CRL 2455	19 44 42.0	+25 05 35	≤0.27	0.0	0.775
CRL 2584	20 25 33.0	+37 12 50	≤0.25	0.0	0.775

* Peak temperature over a 64 MHz spectrometer bandwidth when the instrumental resolution is 0.775 km s^{-1}, or over a 26.5 MHz bandwidth when instrumental resolution is 0.3099 km s^{-1}.

† The spectrometer was centered at 96,747.42 MHz and the indicated Doppler velocity referred to the local standard of rest.

to verify that our radiative transfer model correctly describes the *low-lying* rotational states in methanol.

1. On the observed spectra we superposed Gaussian profiles whose strengths were determined from statistical equilibrium calculations and whose line widths were derived from the data (see Table 2). Figures 1 and 3 show that the computed profiles represent the observed spectra to within the noise.

2. The collision rates used in the calculations (see Table 6) agree to within a factor of 10 with those derived independently from SO data by Gottlieb *et al.* (1978*b*) except in W3(OH).

3. When collision case 1 was used instead of case 2, we obtained column densities that agreed with those in Table 6 to within a factor of 2.

4. We obtained satisfactory agreement between our calculations and the observations of Kutner *et al.* (1973) and Hollis and Ulich (1977), when we used the same kinetic temperature, collision rate, and column density listed in Table 6 to describe the $J = 1 \rightarrow 0$ and $3 \rightarrow 2$ methanol transitions.

ii) *Collision Rates*

For a given source with known kinetic temperature, we adjusted the column density so that the calculated brightness temperature agrees with the measured

TABLE 6

COMPARISON OF CH_3OH AND H_2CO COLUMN DENSITIES

SOURCE	T_k (K)	COLLISION RATE (s^{-1})	TOTAL COLUMN DENSITIES (cm^{-2})* CH_3OH	TOTAL COLUMN DENSITIES (cm^{-2})* H_2CO	H_2CO REFERENCES
W3 (OH)	20	2.4×10^{-5}	1.6 (14)	< 7.0 (14)	1
NGC 1333	20	2.4×10^{-6}	1.0 (14)	2.1 (14)	2
				1.1 (14)	3
Ori A (KL)	60	4.8×10^{-4}	2.4 (15)	1.6–2.9 (14)	4
Ori A (OMC-2)	50	2.4×10^{-5}	6.0 (13)	2.6 (13)	2
NGC 2024	25	2.4×10^{-6}	1.1 (14)	2.3 (13)	5
				2.9 (13)	6
NGC 2264	20	2.4×10^{-6}	4.6 (14)	3.8 (13)	2
ρ Oph	25	2.4×10^{-5}	6.4 (14)	1.6 (13)	2
Sgr A	30	1.2×10^{-5}	3.0 (15)	5.8 (14)	6
Sgr B2	20	2.4×10^{-5}	2.0 (16)	2.2 (15)	6
$^{13}CH_3OH$	20	2.4×10^{-5}	5.0 (14)	...	...
CH_3OD	20	2.4×10^{-5}	9.0 (13)	...	...
M17 SW	50	2.4×10^{-5}	1.5 (14)	6.3 (13)	2
				1.1 (14)	7
W49	10	2.4×10^{-4}	3.0 (14)	7.0 (14)	6
W51	15	2.4×10^{-5}	5.0 (14)	1.6 (14)	6
DR 21 (OH)	25	1.2×10^{-5}	3.2 (14)	4.2 (13)	2
				6.6 (13)	5
NGC 7538	25	1.2×10^{-5}	1.9 (14)	...	...

* Column densities are written with the exponent in parentheses; that is, 1.6×10^{14} is written as 1.6 (14).

REFERENCES.—[1] Evans (private communication); [2] Wootten *et al.* 1979; [3] Lada *et al.* 1974; [4] Kutner *et al.* 1976; [5] Zuckerman *et al.* 1970; [6] Fomalont and Weliachew 1973; [7] Lada 1976.

value of T_A^* in Table 2. We chose the collision rate that gave the correct ratios for the $2_{-1} \rightarrow 1_{-1}\,E$, $2_0 \rightarrow 1_0\,E$, and $2_1 \rightarrow 1_1\,E$ transitions with respect to $2_0 \rightarrow 1_0\,A$. The fact that the collision rates deduced from the CH_3OH spectra agree so closely with those derived independently from SO by Gottlieb *et al.* (1978*b*) demonstrates that a CH_3OH profile obtained with good sensitivity at 96.7 GHz accompanied by a ^{12}CO measurement can yield a collision rate that is independent of calibration problems which otherwise arise when several transitions at different frequencies requiring a retuning of the millimeter wave receiver (e.g., in CS and SO, etc.) are used to derive the collision rate.

When the collision rate is large ($\geq 10^{-4}\ s^{-1}$), as is the case toward the Kleinmann-Low nebula, the $2_1 \rightarrow 1_1\,E$ transition is nearly as strong as $2_0 \rightarrow 1_0\,A$ (see Fig. 1). A large collision rate corresponds to the case when the excitation temperature approaches the kinetic temperature (i.e., LTE). This is why Kutner *et al.* (1973) were able to analyze the $J = 3 \rightarrow 2$ transitions in Orion with an LTE model to obtain a column density similar to the value in Table 6, and were able to reproduce the relative intensities of the transitions they observed. Figure 3 and Table 6 reveal, however, that in most other sources the CH_3OH cannot be correctly analyzed by using an LTE model.

iii) *Results*

The total CH_3OH column densities in 14 sources are listed in Table 6. Spectra of Sgr A, Sgr B2, W49, and W51 were difficult to analyze and the column densities in these sources are uncertain. In Sgr A and Sgr B2 the $2_{-1} \rightarrow 1_{-1}\,E$, $2_0 \rightarrow 1_0\,A$, and $2_0 \rightarrow 1_0\,E$ transitions were unresolved, so information regarding the collision rate is missing. Evidence in § III*a* suggests that $^{12}CH_3OH$ is optically thick in Sgr B2 at 96.7 GHz; therefore we used the $2_1 \rightarrow 1_1\,E$ transition to estimate the column density. In Sgr A the $2_1 \rightarrow 1_1\,E$ transition was too weak to detect, and we guessed the collision rate. In W49 and W51 we used the line widths and collision rates obtained from SO by Gottlieb *et al.* (1978b).

Referring to Table 6, we conclude that in Sgr B2 the abundance ratio[3] $[CH_3OH]/[^{13}CH_3OH]$ is ~ 40, and that the ratio $[CH_3OD]/[CH_3OH]$ is 0.004. In Sgr B2 the $[CH_3OD]/[CH_3OH]$ ratio is within a factor of 2 of the [DCN]/[HCN] ratio determined by Penzias *et al.* (1977), but is 4 times smaller than the $[NH_2D]/[NH_3]$ ratio reported by Turner *et al.* (1978).

The H_2CO column densities are listed for comparison in Table 6. We assumed $T_x = 1.7$ K where necessary to calculate column densities. Where the column density was reported for ortho–H_2CO, we assumed that three-fourths of all H_2CO molecules are in the ortho- state.

Despite its greater complexity, in 11 sources the CH_3OH abundance is comparable to, or greater than, the H_2CO abundance. We are not certain whether the ratio of CH_3OH to H_2CO varies, or whether uncertainties in the column densities are the cause of the apparent variations.

[3] Quantities in square brackets, for example $[CH_3OH]$, refer to abundances.

b) *Comparison with Chemical Formation Theories*

The formation of large polyatomic molecules in dense interstellar clouds is poorly understood. Yet we know from our observations that methanol is very abundant. A formation scheme based on grain-surface reactions (Allen and Robinson 1977) fails to produce significant amounts of methanol. Those advocating the formation of large molecules through gas-phase reactions refer to the semiclassical statistical calculations of Herbst (1976), which indicate that gas-phase radiative association is more efficient for larger molecules.

Smith and Adams (1977) proposed that CH_3OH is formed through radiative association

$$CH_3^+ + H_2O \xrightarrow{k_1} CH_3OH_2^+ + h\nu\,, \qquad (1)$$

followed by dissociative recombination

$$CH_3OH_2^+ + e^- \xrightarrow{k_2} \begin{cases} \xrightarrow{R} CH_3OH + H \\ \xrightarrow{1-R} \text{other products}\,. \end{cases} \qquad (2)$$

Laboratory studies show that CH_3OH is destroyed by reaction with C^+

$$CH_3OH + C^+ \xrightarrow{k_3} CH_2OH^+ + CH\,, \qquad (3)$$

and CH_3^+

$$CH_3OH + CH_3^+ \xrightarrow{k_4} CH_2OH^+ + CH_4\,. \qquad (4)$$

Since the rates for reactions (3) and (4) are nearly the same (Huntress 1977), the principal means of CH_3OH destruction probably depends on whether C^+ or CH_3^+ is more abundant. At steady state,

$$[CH_3OH] = \frac{Rk_1[CH_3^+]}{k_3[C^+] + k_4[CH_3^+]}\,[H_2O]\,. \qquad (5)$$

The principal uncertainty in this formation scheme is the large rate constant required in reaction (1). Smith and Adams (1977) infer an effective two-body rate constant for reaction (1) of $k_1 = 2 \times 10^{-10}$ $cm^3\ s^{-1}$ (Huntress 1977 measured k_3 and k_4). If $[CH_3^+] \sim 0.01[C^+]$ (W. D. Langer and W. T. Huntress, Jr., personal communications), then

$$\frac{[CH_3OH]}{[H_2O]} = (2.43 \times 10^6)k_1R\,.$$

A CH_3OH column density in Orion A of 2×10^{15} cm^{-2} (see Table 6) and an H_2 column density of 10^{24} cm^{-2} (Liszt *et al.* 1974) imply that $[CH_3OH]/[H_2] = 2 \times 10^{-9}$. We obtain an upper limit for k_1R of 8×10^{-8} $cm^3\ s^{-1}$ from the astronomical data if we adopt the $[H_2O]/[H_2]$ ratio calculated by Herbst and Klemperer (1973). We obtain a lower limit of

8×10^{-12} cm^3 s^{-1} for k_1R if we assume that all O is in the form of H_2O. If we adopt the value of 10^{-5} for $[H_2O]/[H_2]$ that Phillips *et al.* (1978) estimated from an analysis of $H_2{}^{18}O$ emission in Orion A, then $k_1R = 8 \times 10^{-11}$ cm^3 s^{-1}. We conclude that the formation scheme for CH_3OH proposed by Smith and Adams (1977) is consistent with the combined CH_3OH and $H_2{}^{18}O$ observations in Orion A.

Methyl alcohol is one of the few molecules detected in interstellar space that has two deuterated forms, CH_2DOH and CH_3OD. Studying CH_2DOH and CH_3OD may help confirm the proposed formation scheme for CH_3OH. The H/D ratios in polyatomic molecules reflect the H/D ratio in the major ionic species (either H_3^+ or HCO^+) in the molecular cloud. Simple proton exchange between H_2D^+ or DCO^+ and CH_3OH will produce CH_3OD but not CH_2DOH (Huntress, personal communication), therefore any D observed as CH_2DOH must have entered during the formation process.

Harrison and Keyes (1973) and Kim, Theard, and Huntress (1974) showed from laboratory studies that the reaction

$$CH_3^+ + HD \xrightarrow{k_6} CH_2D^+ + H_2 + \Delta E_a \quad (6)$$

is very fast ($k_6 = 5 \times 10^{-10}$ cm^{-3} s^{-1}). Watson, Crutcher, and Dickel (1975) estimated that the zero point energy difference for the reaction ΔE_a is more than or equal to 250 K (i.e., the reaction is exothermic). An observation of CH_2DOH with comparable strength to our detection of CH_3OD (see Fig. 2) would provide compelling evidence that reaction (1) involving CH_3^+ is the crucial step in the formation of CH_3OH, since the most plausible way for D to enter CH_2DOH is through the reaction of CH_2D^+ with H_2O

$$CH_2D^+ + H_2O \rightarrow CH_2DOH_2^+ + h\nu\,,$$

$$CH_2DOH_2^+ + e^- \xrightarrow{R} CH_2DOH + H \quad (1-R) \rightarrow \text{other products}\,.$$

c) *A Possible Method for Determining the* H_2O *Abundance*

Herbst *et al.* (1977) summarized the importance and difficulties in determining the H_2O abundance in molecular clouds. If the proposed formation scheme for CH_3OH involving the reaction of CH_3^+ with H_2O is correct, then we can deduce the H_2O abundance in extended molecular clouds from the methanol observations. From equation (5), if $[CH_3^+] \sim 0.01[C^+]$, then

$$[H_2O] = 2 \times 10^3 \times [CH_3OH]/R\,,$$

since $k_1 = 2 \times 10^{-10}$ cm^3 s^{-1} (Smith and Adams 1977), $k_3 = 4.1 \times 10^{-9}$ cm^3 s^{-1}, and $k_4 = 1.4 \times 10^{-9}$ cm^3 s^{-1} (Huntress 1977). When R (the branching ratio of reaction [2]) is measured in the laboratory, the relation between $[H_2O]$ and $[CH_3OH]$ will be quantitatively established provided reaction (1) is the principal source of CH_3OH.

d) *The Relationship between Methanol and Formaldehyde*

The synthesis of formaldehyde (H_2CO) in dense molecular clouds is one of the more perplexing problems confronting astrochemists. Several formation schemes (proposed by Watson and Salpeter 1972; Herbst and Klemperer 1973; Dalgarno, Oppenheimer, and Black 1973; Dalgarno and Black 1976) encountered difficulties when their key reactions were studied in the laboratory (Fehsenfeld, Dunkin, and Ferguson 1974; Huntress 1977). Recently Huntress (personal communication) suggested that H_2CO might be formed from CH_3OH through reaction with either C^+

$$CH_3OH + C^+ \xrightarrow{k_7} CH_2OH^+ + CH\,, \quad (7)$$

or CH_3^+

$$CH_3OH + CH_3^+ \xrightarrow{k_8} CH_2OH^+ + CH_4\,, \quad (8)$$

followed by dissociative recombination

$$CH_2OH^+ + e^- \xrightarrow{k_9} \begin{cases} \xrightarrow{R'} H_2CO + H \\ \xrightarrow{1-R'} \text{other products}\,. \end{cases} \quad (9)$$

The H_2CO is destroyed by either

$$H_2CO + C^+ \xrightarrow{k_{10}} \text{several products} \quad (10)$$

or

$$H_2CO + CH_3^+ \xrightarrow{k_{11}} HCO^+ + CH_4\,. \quad (11)$$

Huntress (1977) measured the rates k_7, k_8, k_{10}, and k_{11}. Because $k_7 \approx k_{10}$ and $k_8 \approx k_{11}$ and because the same molecular ion (either C^+ in reactions [7] and [10], or CH_3^+ in [8] and [11]) is involved in the formation and destruction of the H_2CO, we get the remarkably simple relation

$$[H_2CO] = R' \times [CH_3OH]\,.$$

The branching ratio R' for reaction (9) is not known, but branching ratios for reactions of this type are typically 0.1 to 1. From the astronomical observations of CH_3OH and H_2CO (see Table 6) we find [except possibly for W3(OH)] that $[CH_3OH] \gtrsim [H_2CO]$, implying that $R' \lesssim 1$.

The proposed formation of H_2CO from CH_3OH is consistent with the inferred CH_3OH and H_2CO abundances. A comparison of the angular distribution of CH_3OH and H_2CO would help confirm the proposed H_2CO formation scheme. If H_2CO is formed primarily from CH_3OH, then the angular distributions of the two should agree.

From our observations of the molecular clouds in Orion (§ III*c*) and those near the galactic-center region (§ III*d*), and from the general ubiquitousness of the methanol as demonstrated by our survey at 96.7 GHz (see Table 2), we feel that CH_3OH is as widely distributed as H_2CO. The notion that CH_3OH and H_2CO are intimately related through their chemistry is at least not contradicted by our observations.

V. SUMMARY

We observed $^{12}CH_3OH$ toward 14 sources at 96.7 GHz. The peak strength of the emission is less than or ~ 1 K, except toward the Kleinmann-Low nebula, Sgr A, and Sgr B2, where it is 2 or 3 K.

We detected $^{13}CH_3OH$ and CH_3OD toward Sgr B2 and set an upper limit for $^{13}CH_3OH$ toward Orion A.

We detected $^{12}CH_3OH$ at 834 MHz toward nine positions in the galactic-center region. The CH_3OH emission is extended with respect to the $\sim 40'$ telescope beamwidth. The number of CH_3OH molecules peak near Sgr A and Sgr B2 where the optical depth is $\sim 10^{-3}$. The CH_3OH emission at 36 cm and the H_2CO absorption at 6 cm (Scoville, Solomon, and Thaddeus 1972) are comparable in extent.

$^{12}CH_3OH$ is probably optically thick in Sgr B2 at 96.7 GHz, but in other sources we treated the spectra satisfactorily with the optically thin case. The CH_3OH column densities are $\sim 2 \times 10^{16}$ cm^{-2} toward Sgr B2, $\sim 3 \times 10^{15}$ cm^{-2} toward Sgr A (3'S), $\sim 2 \times 10^{15}$ cm^{-2} toward the Kleinmann-Low nebula, and $\lesssim 6 \times 10^{14}$ cm^{-2} toward the other sources.

CH_3OH is more abundant than H_2CO.

We estimate that in Sgr B2 the abundance ratio $[^{12}CH_3OH]/[^{13}CH_3OH]$ is ~ 40, and that the ratio $[CH_3OD]/[^{12}CH_3OH]$ is 0.004.

$^{12}CH_3OH$ spectra at 96.7 GHz with better sensitivity will yield precise estimates of the collision rate.

A scheme involving the reaction of CH_3^+ with H_2O to form CH_3OH (Smith and Adams 1977) is consistent with observations.

We thank the staff of the National Radio Astronomy Observatory for their help with the observations. We are especially grateful to Dr. M. M. Litvak for computing the methanol line strengths, for the use of his statistical equilibrium program, and for numerous helpful discussions. We are grateful to Professor R. M. Lees for computing the CH_3OD frequencies and to Dr. Richard Suenram and Dr. Frank Lovas for subsequently measuring the CH_3OD frequencies in the laboratory, to Professor Neal J. Evans II for communicating unpublished H_2CO column densities, and to Dr. W. T. Huntress, Jr. for discussions of methanol formation. Ms. Barbara Smith Moran assisted with the 834 MHz observations, and Mrs. S. K. Rosenthal assisted with the calculations. We thank Professor W. Liller for permission to use the Mann measuring engine, and Mr. Phil Pinto for assistance in digitizing the spectra. This work was supported in part by NSF grant MPS 74-24063.

REFERENCES

Allen, M., and Robinson, G. W. 1977, *Ap. J.*, **212**, 396.
Ball, J. A., Gottlieb, C. A., Lilley, A. E., and Radford, H. E. 1970, *Ap. J.* (*Letters*), **162**, L203.
Barrett, A. H., *et al.* 1976, *Ap. Letters*, **18**, 13.
Barrett, A. H., Martin, R. N., Myers, P. C., and Schwartz, P. R. 1972, *Ap. J.* (*Letters*), **178**, L23.
Buxton, R. B., Barrett, A. H., Ho, P. T. P., and Schneps, M. H. 1977, *A.J.*, **82**, 985.
Dalgarno, A., and Black, J. H. 1976, *Rept. Progr. Phys.*, **39**, 573.
Dalgarno, A., Oppenheimer, M., and Black, J. H. 1973, *Nature Phys. Sci.*, **245**, 100.
Fehsenfeld, F. C., Dunkin, D. B., and Ferguson, E. E. 1974, *Ap. J.*, **188**, 43.
Fomalont, E. B., and Weliachew, L. 1973, *Ap. J.*, **181**, 781.
Gottlieb, C. A., Gottlieb, E. W., Litvak, M. M., and Ball, J. A. 1978*a*, in preparation.
Gottlieb, C. A., Gottlieb, E. W., Litvak, M. M., Ball, J. A., and Penfield, H. 1978*b*, *Ap. J.*, **219**, 77.
Gottlieb, C. A., Lada, C. J., Gottlieb, E. W., Lilley, A. E., and Litvak, M. M. 1975, *Ap. J.*, **202**, 655.
Harrison, A. G., and Keyes, B. G. 1973, *Canadian J. Chem.*, **51**, 1265.
Herbst, E. 1976, *Ap. J.*, **205**, 94.
Herbst, E., and Klemperer, W. 1973, *Ap. J.*, **185**, 505.
Herbst, E., Green, S., Thaddeus, P., and Klemperer, W. 1977, *Ap. J.*, **215**, 503.
Hills, R., Pankonin, V., and Landecker, T. L. 1975, *Astr. Ap.*, **39**, 149.
Hollis, J. M., and Ulich, B. L. 1977, *Ap. J.*, **214**, 699.
Huntress, W. T., Jr. 1977, *Ap. J. Suppl.*, **33**, 495.
Kim, J. K., Theard, L. P., and Huntress, W. T., Jr. 1974, *J. Chem. Phys.*, **62**, 45.
Kutner, M. L., Evans, N. J., II, and Tucker, K. D. 1976, *Ap. J.*, **209**, 452.
Kutner, M. L., Thaddeus, P., Penzias, A. A., Wilson, R. W., and Jefferts, K. B. 1973, *Ap. J.* (*Letters*), **183**, L27.
Lada, C. J. 1976, *Ap. J. Suppl.*, **32**, 603.
Lada, C. J., Gottlieb, C. A., Litvak, M. M., and Lilley, A. E. 1974, *Ap. J.*, **194**, 609.
Lees, R. M. 1973, *Ap. J.*, **184**, 763.
Lees, R. M., Lovas, F. J., Kirchhoff, W. H., and Johnson, D. R. 1973, *J. Phys. Chem. Ref. Data*, **2**, 205.
Liszt, H. S., Wilson, R. W., Penzias, A. A., Jefferts, K. B., Wannier, P. G., and Solomon, P. M. 1974, *Ap. J.*, **190**, 557.
Penzias, A. A., Wannier, P. G., Wilson, R. W., and Linke, R. A. 1977, *Ap. J.*, **211**, 108.
Phillips, T. G., Scoville, N. Z., Kwan, J., Huggins, P. J., and Wannier, P. G. 1978, *Ap. J.* (*Letters*), **222**, L59.
Scoville, N. Z., Solomon, P. M., and Jefferts, K. B. 1974, *Ap. J.* (*Letters*), **187**, L63.
Scoville, N. Z., Solomon, P. M., and Thaddeus, P. 1972, *Ap. J.*, **172**, 335.
Smith, D., and Adams, N. G. 1977, *Ap. J.*, **217**, 741.
Solomon, P. M., Scoville, N. Z., Penzias, A. A., Wilson, R. W., and Jefferts, K. B. 1972, *Ap. J.*, **178**, 125.
Turner, B. E., Gordon, M. A., and Wrixon, G. T. 1972, *Ap. J.*, **177**, 609.
Turner, B. E., Zuckerman, B., Morris, M., and Palmer, P. 1978, *Ap. J.* (*Letters*), **219**, L43.
Wannier, P. G., Arnaud, J. A., Pelow, F. A., and Saleh, A. A. M. 1976, *Rev. Sci. Instr.*, **47**, 56.
Watson, W. D., and Salpeter, E. E. 1972, *Ap. J.*, **175**, 659.
Watson, W. D., Crutcher, R. M., and Dickel, J. R. 1975, *Ap. J.*, **201**, 102.
Wooten, H. A., Snell, R., and Evans, N. J., II. 1979, *Ap. J.*, in press.
Zuckerman, B., Buhl, D., Palmer, P., and Snyder, L. E. 1970, *Ap. J.*, **160**, 485.
Zuckerman, B., Turner, B. E., Johnson, D. R., Palmer, P., and Morris, M. 1972, *Ap. J.*, **177**, 601.

JOHN A. BALL, C. A. GOTTLIEB, and ELAINE W. GOTTLIEB: Harvard-Smithsonian Center for Astrophysics, 60 Garden Street, Cambridge, MA 02138

DALE F. DICKINSON: Physics and Astronomy Department, Williams College, Williamstown, MA 01267